



## Radiation resistance of photodiodes based on indium monoselenides under $\gamma$ -irradiation

Z.D. Kovalyuk<sup>a,\*</sup>, O.A. Politsanska<sup>a</sup>, V.G. Tkachenko<sup>b</sup>, I.N. Maksymchuk<sup>b</sup>, V.V. Dubinko<sup>c</sup>, A.I. Savchuk<sup>d</sup>

<sup>a</sup>Chernivtsi Department of the Institute of Materials Science Problems, The National Academy of Sciences of Ukraine, 5, Iryna Vilde Str., 58001 Chernivtsi, Ukraine

<sup>b</sup>Institute of Materials Science Problems, The National Academy of Sciences of Ukraine, Krzhizhanivskogo Str., 3, 03680 Kyiv, Ukraine

<sup>c</sup>National Scientific Center "Kharkiv Physico-Technical Institute", The National Academy of Sciences of Ukraine, 1, Academichna Str., 61108 Kharkiv, Ukraine

<sup>d</sup>Chernivtsi National University, 2, Kotsyubynsky Str., 58012 Chernivtsi, Ukraine

### ARTICLE INFO

PACS:  
61.80.Ed  
61.82.Fk  
73.40.-c  
73.40.Lq

### ABSTRACT

The influence of  $\gamma$ -irradiation ( $E = 3$  MeV) over a large dose range 0.14–140 kGy on the electrical and photoelectric parameters of p–n–InSe and *intrinsic oxide*–p–InSe photoconvertors has been investigated. The detected changes in current–voltage characteristics, photoresponse spectra, open-circuit voltage, and short-circuit current for the structures are explained by the formation of radiation-induced point defects. A comparison to silicon photodiodes irradiated at analogous conditions has been carried out. On the basis of the absence of essential changes of the characteristics of the homo- and hetero-junctions based on III–VI layered semiconductors even at the maximum irradiation doses these junctions are recommended as radiation-resistant photodetectors for operation under  $\gamma$ -irradiation.

© 2008 Elsevier B.V. All rights reserved.

### 1. Introduction

Limited studies have been performed of the influence of penetrating radiation on anisotropic layered III–VI semiconductors. Such studies are needed to allow their electronic properties to be predicted and to establish the behaviour of homo- and hetero-structures based on layered crystals. Such structures show extraordinary promise for creation of high-efficient radiation-resistant photoconvertors and semiconductor detectors for nuclear radiations and particles. In comparison to other semiconductors (Si, Ge, GaAs and InP), layered crystals have higher resistance to hard radiations (high-energy electrons and neutrons,  $\gamma$ -ray photons), as essential changes to their electrical parameters begin at comparatively high irradiation doses [1,2]. Moreover, the photoelectric parameters of InSe-based diodes actually improve under the influence of small doses of  $\gamma$ -irradiation [3,4]. Intentionally-doped, high-resistive layered crystals enable creation of high-sensitive radiation detectors [5,6] providing an alternative to the current widespread use of CdTe.

Only a few studies have been conducted on the radiation resistance of layered III–VI semiconductor crystals and those that have are restricted to  $\gamma$ -irradiation [7–10]. Similarly, only a few publications have examined the influence of  $\gamma$ -irradiation on the properties of InSe-based photodiodes [3,4,11].  $\gamma$ -Irradiation with energy  $E = 1.33$  MeV was carried out by means of radioactive  $^{60}\text{Co}$  cobalt

isotope only in the negligible dose range (between 0.1 and 3 Gy) [3,4]. The results presented by Aliev et al. [11] only examined photoelectric properties for a single type of structure – Schottky-barrier diode Au–n–InSe. Therefore, complex investigations of electrical and photoelectric characteristics of several types of photoconvertors based on layered crystals over a wide range of  $\gamma$ -photon doses are needed.

The behaviour of p–InSe:Cd–n–InSe and *intrinsic oxide*–p–InSe photosensitive structures subject to bremsstrahlung  $\gamma$ -radiation with a dose ranging from 0.14 to 140 kGy are described in this study and compared with silicon photodiodes irradiated under similar conditions.

### 2. Experimental procedures

InSe single crystals were grown by the vertical Bridgman method. Intentionally undoped InSe had n-type conductivity with a concentration of uncompensated donors of  $10^{14}$ – $10^{15}$   $\text{cm}^{-3}$  and a Hall mobility along the layers  $\mu_n = 10^3$   $\text{cm}^2 \text{V}^{-1} \text{s}^{-1}$  at 300 K. For obtaining p-type conductivity indium monoselenide was doped with 0.2 wt% Cd what leads to the following parameters:  $p = 10^{13}$   $\text{cm}^{-3}$  and  $\mu_p = 10^2$   $\text{cm}^2 \text{V}^{-1} \text{s}^{-1}$ . The grown single crystals had a well pronounced layered structure and mirror-like cleaved surfaces.

Homo-junctions p–n–InSe were prepared by means of direct optical contact [12]. Thin ( $\sim 10$ – $50$   $\mu\text{m}$ ) plates of InSe:Cd were used as a front-face semiconductor. InSe plates of a 250–300  $\mu\text{m}$  thickness were applied as a base substrate. *Intrinsic oxide*–p–InSe surface-barrier diodes were produced by thermal oxidation of indium

\* Corresponding author. Tel.: +38 0372 525155; fax: +38 0372 236018.  
E-mail address: [chimsp@ukrpost.ua](mailto:chimsp@ukrpost.ua) (Z.D. Kovalyuk).

selenide substrates in air [13]. The applied technologies are simpler than those usually applied and use a practical diffusion technique making it possible to manufacture structures with shallow location of the p–n-junctions. Specific parameters of the homo- and hetero-junctions were high and reproducible. The area of the photodiodes was about 0.25 cm<sup>2</sup>. The electric contacts were formed by soldering pure indium.

For comparison a wide-gap semiconductor – tunnel dielectric – semiconductor hetero-junction In<sub>2</sub>O<sub>3</sub>–SiO<sub>2</sub>–n-Si was investigated.

The samples have been  $\gamma$ -irradiated at a linear electron accelerator KUT-10. The technique of producing a secondary beam of  $\gamma$ -photon was as follows. As the 10 MeV electron beam passes through a tantalum converter, it generates bremsstrahlung  $\gamma$ -photon in the energy range of 0.5–11.5 MeV with a maximum at 3 MeV. Electron component in the output beam did not exceed 5%. The flux of  $\gamma$ -photon was about  $2 \times 10^{11}$  cm<sup>-2</sup> s<sup>-1</sup>, and the irradiation time was chosen so that to give the total  $\gamma$ -fluence,  $\Phi = 2 \times 10^{13}$ – $2 \times 10^{16}$  cm<sup>-2</sup> that corresponds to the absorbed dose,  $D = 0.14$ – $140$  kGy. The temperature of the samples under irradiation did not exceed 297 K.

The current–voltage ( $I$ – $V$ ) and capacitance–voltage ( $C$ – $V$ ) characteristics and the impedance spectra were measured by using a Schlumberger SI 1255 & 1286 amplitude–frequency analyzer. The device allowed measuring currents of the order of  $10^{-10}$  A. For the measurements structures were placed in a screened chamber. Results were analysed by means of the ‘ZView 2.4a’ and ‘CView 2.4a’ software. The parameters of the structures (open-circuit voltage  $V_{oc}$ , short-circuit current density  $J_{sc}$ ) under illumination were investigated to an accuracy of 0.5% by using a standard stand. A 200 W tungsten lamp with a parabolic reflector was applied as the light source. The incident radiation power was measured by a calibrated Si solar cell and equal to  $\sim 100$  mW cm<sup>-2</sup>. The photosensitivity spectra were measured by using a MDR-23 grating monochromator with a resolution not worse than 1 meV. The spectral distribution of the relative quantum efficiency of photoconversion was determined as the ratio of photocurrent to number of incident photons. Monochromatic current–watt (volt–watt) sensitivities were calculated as the ratio of photocurrent (photovoltage) to power of monochromatic radiation fluence at a wavelength  $\lambda = 0.98$   $\mu$ m, which has caused the appearance of this photocurrent (photovoltage).

X-ray diffraction (XRD) investigations of the samples were made in monochromatic CuK $\alpha$ -radiation with a DRON-UM1 diffractometer. A black lead single crystal mounted on the path of a diffracted beam was used as monochromator. Precise measurements of the lattice parameters were carried out by the Bond method from the measured angular distances between the symmetric reflecting positions of the crystal: reflections 200 and 110 for the parameter  $a$  with an accuracy of  $\pm 0.0001$  nm (to within  $\pm 0.0001$  nm) and a reflection 0018 for the parameter  $c$  with an accuracy of  $\pm 0.0002$  nm.

Raman spectra of the crystals were excited by an argon laser with a wavelength of 514.5 nm and registered by a spectrometer DFS-24.

All measurements were carried out at room temperature.

### 3. Results and discussion

#### 3.1. XRD measurements

XRD of the initial InSe and InSe:Cd crystals before (Figs. 1(a) and 2(a)) and after (Figs. 1(b) and 2(b)) irradiation with a dose 140 kGy confirms that in all the states these crystals are single phase InSe of the 3R rhombohedral structure. The measurements of the unit cell parameters by using the Bond method at 110 and 0027 reflections

are listed in Table 1 and indicate the  $\gamma$ -polytype of indium selenide (space group  $C_{3v}^5$ ). A typical feature of the XRD spectra for the samples under investigation is the presence of diffusion maxima nearby the 009, 00.12, and 00.18 peaks of the 3R structure. These peaks are situated from the side of smaller angles and can be interpreted as caused by stacking faults in the 3R structure, which lead to stacking of the layers typical for the 2H structure of InSe (the space group  $D_{6h}^4$ ). Figs. 1 and 2 reveal no essential changes in the crystals after irradiation with  $\gamma$ -photon except for a small decrease of the lattice parameters (see Table 1). The InSe lattice is thus highly resistant to  $\gamma$ -radiation even for the bond combination in this layered compound: strong ionic – covalent bonding within the layers and weak Van der Waals forces between them.

#### 3.2. Raman spectra measurements

The Raman spectra of InSe and InSe:Cd crystals in the initial state (Fig. 3(a) and (b), respectively) are very similar each other, except for a small transferring intensity between the two bands in the range of 215 and 230 cm<sup>-1</sup>. Note that in the InSe:Cd sample the band at 215 cm<sup>-1</sup>, which is caused by the presence of Cd atoms, is better expressed (Fig. 3(b)). The Raman spectra of the irradiated n-InSe and InSe:Cd crystals contain the bands at frequencies 120.8, 184.8, 205.7, 218.0, 231.8, 409.3, and 430.3 cm<sup>-1</sup> (Fig. 3(c) and (d)). These bands correspond to those known from the literature Raman spectra of InSe [14]. Insignificant transfer of relative intensities between the bands in the spectra of different samples was observed. This is caused by different defect concentrations in these samples after their irradiation. Other peculiarities related to a change of atoms coordination were not found. Thus, irradiation of the layered crystals has not led to qualitative changes in the investigated

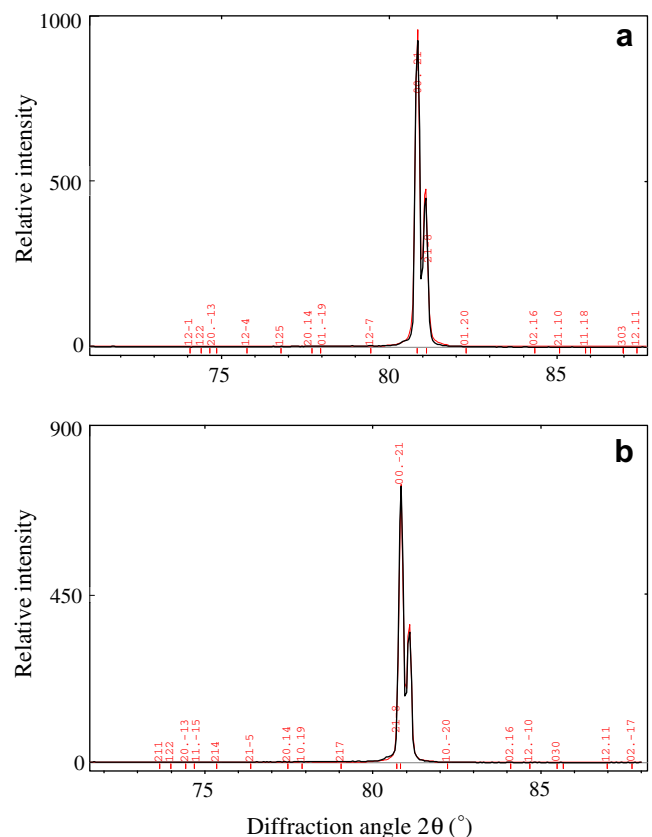


Fig. 1. XRD spectra (selected part) of the initial InSe single crystal (a) and irradiated (b) with a maximum dose.

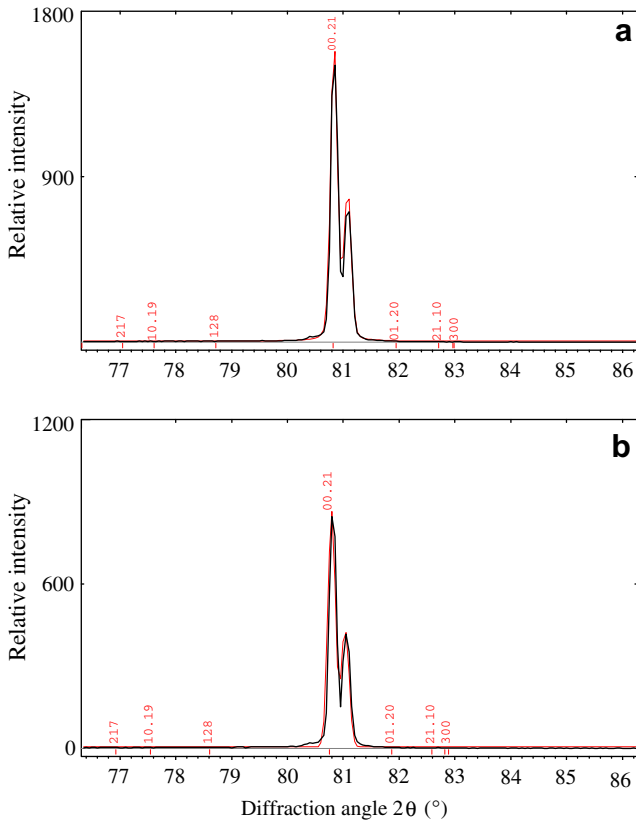


Fig. 2. XRD spectra (selected part) of the initial InSe:Cd single crystal (a) and irradiated (b) with a maximum dose.

**Table 1**  
The lattice parameters of InSe and InSe:Cd single crystal with rhombohedral crystal structure before and after irradiation with maximum dose.

Lattice parameter (nm)	Unirradiated samples		Irradiated samples	
	a	c	a	c
InSe	0.4003	2.4960	0.4002	2.4950
InSe:Cd	0.4003	2.4969	0.4003	2.4949

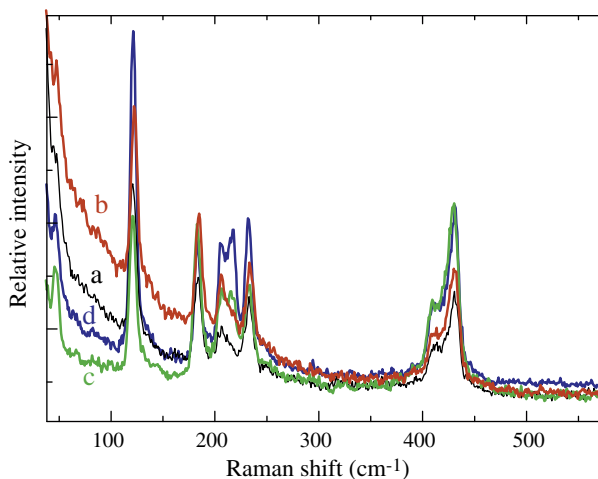


Fig. 3. Raman spectra of unirradiated InSe (a) and InSe:Cd (b) single crystals and also irradiated with a maximum dose InSe (c) and InSe:Cd (d) single crystals.

Raman spectra which are extremely sensitive to variation of the coordination of Raman scattering centres. This makes layered semiconductors attractive from the point view of radiation hardness. The conclusion about insignificant influence of irradiation with  $\gamma$ -photon at fluences up to  $5 \times 10^{15} \text{ cm}^{-2}$  on a change of the vacancy and impurity subsystems in layered InSe crystals has been indirectly confirmed by the authors of [15].

### 3.3. Electrical measurements

The dynamics of the change of the  $J$ - $V$  characteristics with irradiation are shown in Figs. 4 and 5. The initial parts of all the  $J$ - $V$  characteristics can be described by an exponential dependence [16]:

$$J = J_s [\exp(qV/nkT) - 1]. \quad (1)$$

Here  $J$  is current density,  $T$  is the absolute temperature,  $k$  is the Boltzmann constant,  $n$  is the diode ideality factor,  $q$  is the elementary charge and  $J_s$  is a saturation current density. However, at forward biases above 0.3 V the experimental points do not agree

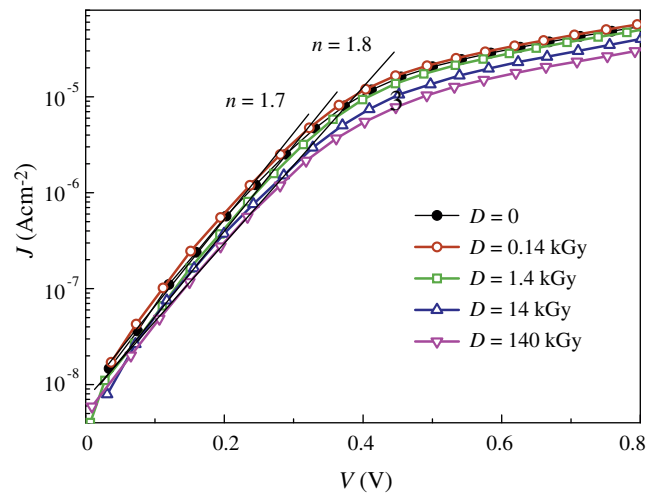


Fig. 4. Forward branches of  $J$ - $V$  curves for p-n-InSe homo-junction irradiated with different fluences. Straight lines correspond to the  $J = \exp[q(V-IR_s)/nkT]$  dependence.  $T = 293$  K.

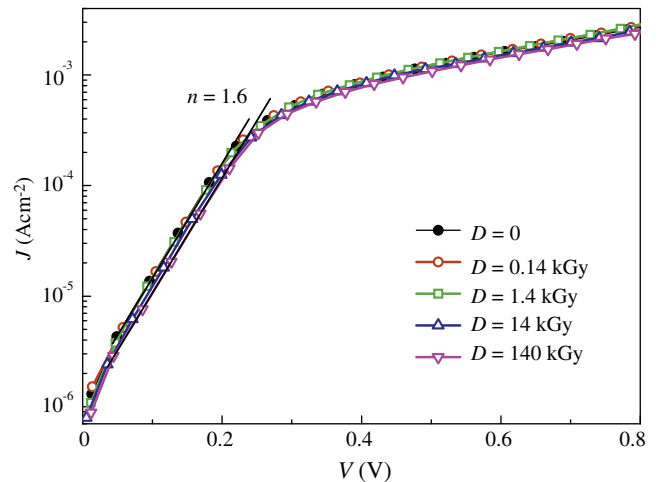


Fig. 5. Forward branches of  $J$ - $V$  curves for intrinsic oxide-p-InSe hetero-structure irradiated with different doses. Straight lines correspond to the  $J = \exp[q(V-IR_s)/nkT]$  dependence.  $T = 293$  K.

with this dependence which is caused by a redistribution of the voltage drop between the barrier and quasi-neutral ranges of the structure. Therefore, at high current densities the  $J$ - $V$  characteristics reflect mainly charge transfer through a series resistance  $R_s$  but not the real mechanism of charge transfer through the potential barrier. The value of  $R_s$  (see Table 2) was established from impedance measurements of the structures. It enabled the  $J$ - $V$  characteristics to be replotted as functions of voltage drop  $V - IR_s$  at the barrier part of the diode instead of applied voltage  $V$ . The results of such replotting of the experimental data are shown in Figs. 4 and 5 by straight lines. The voltage drop, taking into account  $R_s$ , essentially changes the experimental curves and yields to the equation:

$$J = J_s \{ \exp[q(V - IR_s)/nkT] - 1 \} \quad (2)$$

Now the part corresponding to dependence Eq. (2) becomes longer. This portion was used to determine the diode coefficient  $n$  from the relation:

$$n = \frac{q}{kT} \frac{\Delta V}{\Delta \ln J} \quad (3)$$

As a result, with irradiation there is a slight change of the exponential current vs voltage dependence and, therefore, keeping the over-barrier ( $n = 1.6$ – $1.8$ ) charge transfer mechanism (see Table 2). It is known that except for the diffusive component in real structures there are shunting currents [1,2,17]. This explains that  $n > 1$  for unirradiated InSe-diodes. On the other hand, high-energy radiation creates structure defects which increase the density of recombination centres in the space-charge region of the p-n transition. As a result, recombination currents worsen the diode coefficient of the  $J$ - $V$  characteristics increase. For the investigated structures a small increase of  $n$  at the maximum irradiation fluence proves that the number of radiation-induced defects is fewer than the number of intrinsic defects in the layered crystals.

**Table 2**  
Variation of electrical and photoelectric parameters of InSe photodiodes before and after irradiation (all data in the table are rounded to the last digit).

Fluence (Gy)	0	0.14	1.4	14	140
<i>Homo-junction p-n-InSe</i>					
$K$ for $ V  = 1$ V	100	105	135	185	210
$n$	1.7	1.7	1.7	1.8	1.8
$V_{oc}$ (V)	0.49	0.52	0.53	0.55	0.54
$J_{sc}$ (mA cm <sup>-2</sup> )	0.41	0.43	0.41	0.38	0.37
$S$ (eV <sup>-1</sup> )	39	55	57	54	53
$S_i$ at $\lambda = 0.98$ $\mu$ m (mA W <sup>-1</sup> )	49	73	83	87	89
$S_V$ at $\lambda = 0.98$ $\mu$ m (V W <sup>-1</sup> )	$3.7 \times 10^4$	$3.9 \times 10^4$	$4.0 \times 10^4$	$4.2 \times 10^4$	$4.1 \times 10^4$
$R_s$ ( $\Omega$ cm <sup>2</sup> )	$9.0 \times 10^3$	$8.5 \times 10^3$	$9.1 \times 10^3$	$9.7 \times 10^3$	$1.0 \times 10^4$
$R_{sh}$ ( $\Omega$ cm <sup>2</sup> )	$1.3 \times 10^6$	$1.5 \times 10^6$	$2.3 \times 10^6$	$2.7 \times 10^6$	$3.1 \times 10^6$
<i>Hetero-junction intrinsic oxide-p-InSe</i>					
$K$ for $ V  = 1$ V	292	335	370	316	285
$N$	1.6	1.6	1.6	1.6	1.6
$V_{oc}$ (V)	0.58	0.58	0.59	0.58	0.58
$J_{sc}$ (mA cm <sup>-2</sup> )	5.1	5.5	5.6	5.0	5.0
$S$ (eV <sup>-1</sup> )	44	61	67	69	68
$S_i$ at $\lambda = 0.98$ $\mu$ m (mA W <sup>-1</sup> )	110	123	130	141	144
$S_V$ at $\lambda = 0.98$ $\mu$ m (V W <sup>-1</sup> )	$1.8 \times 10^4$	$2.0 \times 10^4$	$2.3 \times 10^4$	$2.6 \times 10^4$	$2.6 \times 10^4$
$R_s$ ( $\Omega$ cm <sup>2</sup> )	215	200	195	224	228
$R_{sh}$ ( $\Omega$ cm <sup>2</sup> )	$2.2 \times 10^4$	$2.6 \times 10^4$	$2.9 \times 10^4$	$3.0 \times 10^4$	$3.1 \times 10^4$
<i>Hetero-junctions In<sub>2</sub>O<sub>3</sub>-SiO<sub>2</sub>-n-Si</i>					
$V_{oc}$ (V)	0.52	–	–	0.49	0.45
$J_{sc}$ (mA cm <sup>-2</sup> )	15.3	–	–	10.7	7.3
$S_i$ at $\lambda = 0.98$ $\mu$ m (mA W <sup>-1</sup> )	150	–	–	36	17
$S_V$ at $\lambda = 0.98$ $\mu$ m (V W <sup>-1</sup> )	$1.2 \times 10^4$	–	–	$6.3 \times 10^3$	$2.0 \times 10^3$

The power dependence of the current vs voltage profile  $J_{\infty}V^m$  is typical for reverse currents. In the range of reverse biases 0–5 V the exponent  $m$  in series takes a value from 1 to 3. Such behaviour of the  $J$ - $V$  characteristics of neutral ranges is typical for space-charge limited current [18] and has been observed for InSe single crystals [19] and structures based on it [1,2]. In general, there is a common tendency to insignificant variations in the field dependence of reverse currents related to a change of the series resistance of the substrate with irradiation.

Also, for both types of investigated structures the p-n-junctions show improved quality because of the positive tendency of increasing shunting resistances  $R_{sh}$  (see Table 2) with irradiation.

On the whole, the  $J$ - $V$  characteristics show a high degree of p-n transition resistance under irradiation: the current rectification coefficients  $K$  improve slightly during irradiation (see Table 2). The basic cause of this is a behaviour of reverse currents, which decrease substantially with increasing  $\gamma$ -photon dose at a less degree of the change of direct currents.

To determine the irradiation-induced variations in both the potential barrier height and the concentration of ionized acceptors,  $C$ - $V$  characteristics were studied for the p-n-InSe and *intrinsic oxide*-p-InSe structures. In the  $1/C^2$ - $V$  coordinates these characteristics were linear before irradiation which indicates that the p-n junction is abrupt. In addition, the characteristics were dependent of testing signal frequency. Such behaviour is caused by the effect of the hetero-junction's series resistance  $R_s$  on the measurements of capacitance [20]. The full agreement of the behaviour of open-circuit voltage  $V_{oc}$ , short-circuit current  $J_{sc}$  of the structures, height of the potential barrier and acceptor concentration with the course of irradiation was obtained.

### 3.4. Photoelectric measurements

For the p-n-InSe homo-junction a spectral dependence of photoconversion quantum efficiency  $\eta$  covers the photon energy range 1.2–3 eV with a maximum at  $\sim 1.5$  eV for the unirradiated structure (Fig. 6). The presence of such a maximum is due to competitive contributions of the bulk and surface recombination. The energy position of the long-wavelength edge of the spectrum of quantum efficiency  $\eta(h\nu)$  observed at  $h\nu = 1.24$  eV corresponds to the InSe energy gap. The long-wavelength increase of the  $\eta = f(h\nu)$  dependence can be compared to the slope  $S = \Delta(\ln \eta)/\Delta h\nu$  (see Table 2). The photosensitivity increase for

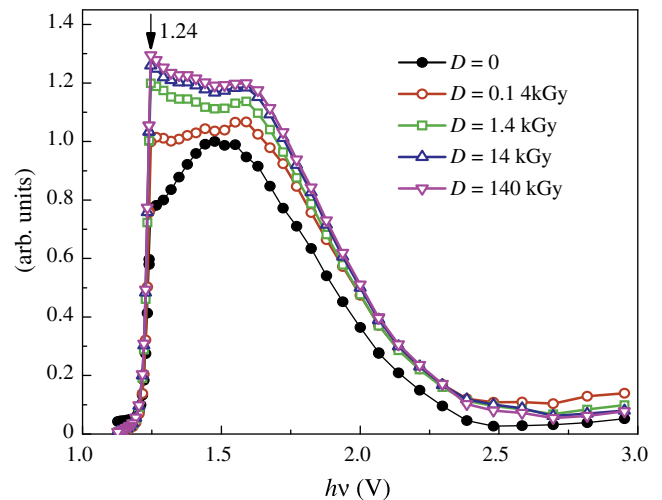


**Fig. 6.** Room temperature spectra of photoconversion quantum efficiency  $\eta$  for p-n-InSe homo-junctions irradiated with different doses.

$h\nu \geq 1.2$  eV is related to a monotonous increase of the absorption coefficient [16]. The spectra also exhibit rather atypical short-wavelength decay in some energy range of light quanta at  $h\nu > 2.0$  eV, which is related to a relatively large depth of the p–n junction.

At an irradiation dose of  $D = 0.14$  Gy and in the photon energy range below the energy of the InSe band-to-band transitions ( $E = 1.24$  eV), the photoresponse curves show a significant increase of photocurrent, which is created by participation of exciton transitions, and the exciton peak appears at dose  $D = 1.4$  Gy (Fig. 6). An increase of exciton absorption intensity in the optical spectra of InSe doped with rare-earth elements Er [21] and Dy [22] is explained by a result of reduction of the number of structural defects in these crystals. In this case it is possible also to talk about some increase of the degree of layer stacking ordering (intrinsic structural defects) in InSe single crystals and an increase of the dissociation of excitons that results in increasing photosensitivity of the structures. A comparison of the photoresponse spectra of the homo-junctions irradiated with doses 1.4–140 Gy shows that there are no any variations in the energy position or form of the spectra. The change is only in the absolute photocurrent values. Accordingly, the monochromatic volt–watt ( $S_V$ ) and current–watt ( $S_I$ ) sensitivities becomes higher (see Table 2). The constant shape of the  $\eta(h\nu)$  spectra indicates on the absence of degradation of the p–n–InSe homo-junction under action of the penetrating radiation.

The *intrinsic oxide*–p–InSe structures are shown in Fig. 7 and have the shape of a band limited on both sides as is typical for spectra of hetero-junctions. The photosensitivity long-wavelength edge at  $\sim 1.2$  eV is caused by the absorption of light in the base semiconductor while the short-wavelength edge (at the photon energy  $h\nu \geq 2.0$  eV) is because of the absorption in the intrinsic oxide film [13]. A low photosensitivity at  $h\nu > 2.0$  eV is explained by the small thickness of the oxide layer.

The spectra of the *intrinsic oxide*–p–InSe hetero-junction reveals a noticeable peak in the long-wavelength range (at the photon energy  $h\nu = 1.25$  eV) corresponding to the excitonic absorption of light in InSe. It is known that the fine structure of excitonic spectra is not observed in the case of imperfect crystals. In this case the excitonic peak intensity is unchanged with increasing irradiation time, which indicates that the structure of the layered semiconductor is retained against the background of introduced radiation defects. When compared with the unirradiated structure, the photocurrent quantum efficiency for the irradiated *intrinsic oxide*–p–InSe hetero-junctions changes practically to the same extent in the whole range of photon energies.

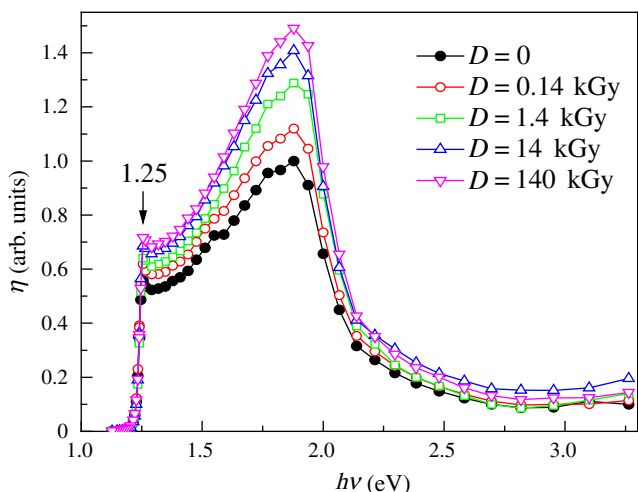


Fig. 7. Room temperature spectra of photoconversion quantum efficiency  $\eta$  for *intrinsic oxide*–p–InSe hetero-structures irradiated with different doses.

The obtained results can be summarized as follows. Although a large number of possible interaction mechanisms are known for gamma-rays in matter, only three major types play an important role in our case: photoelectric absorption, Compton scattering, and pair production. All these processes lead to the partial or complete transfer of the gamma-ray photon energy to electron energy. They result in sudden and abrupt changes in the gamma-ray photon history, in that the photon either disappears entirely or is scattered through a significant angle. Owing to the peculiarities of chemical bonds in layered crystals, the low threshold for formation of defects is sufficient for  $\gamma$ -ray photons to become the reason for generation of defects. Therefore, a classical pattern of the appearance of appreciable concentration of defects, mainly non-equilibrium Frenkel pairs, is observed on irradiation with  $\gamma$ -photons. They can be considered as spatial distributions of simple point defects. With increasing radiation dose there is an increase and subsequent stopping the quantum efficiency increase what is caused by the appearance of radiative and non-radiative recombination centres at the maximum fluences. In InSe crystals the vacancies of indium atoms and chalcogenide atoms in the interstitials are elementary defects whereas defects including selenium atoms and intrinsic lattice defects in the form of a neutral bivacancy  $V_{In}$  ( $V_{Ga}$ ) and  $V_{Se}$  are complex clusters. The latter are responsible for non-radiative recombination centres being accumulated with increasing irradiation. The role of photosensitivity centres is played by chalcogenide vacancies in these semiconductors. Indeed, defects induced by  $\gamma$ -irradiation of GaSe contain selenium vacancies  $V_{Se}$  as explained by the specific features of the GaSe layered structure, which provides for weak coupling of selenium in the lattice [9].

The irradiation fluences used in this work would induce strong degradation on the parameters of conventional Si-based photodiodes. Photosensitivity of  $In_2O_3$ – $SiO_2$ –n–Si structures due to irradiation with  $\gamma$ -photon at maximal dose of 140 Gy decreases by 89% whereas InSe-based photodiodes show the increase of  $S_I$  value by 31% (see Table 2). The same applies to the values of  $V_{oc}$  and  $J_{sc}$ : for the Si structure where equivalent decreases of 13% and 52% were detected. At the same time layered photodiodes have demonstrated a stability or increase of these parameters (see Table 2).

#### 4. Conclusions

It was stated that the structures based on layered InSe crystals under  $\gamma$ -irradiation did not only lose but improved their electrical and photoelectrical characteristics. For the investigated photodiodes the  $\gamma$ -photon (for  $E = 3$  MeV) doses were not sufficient for essential transformations in the intrinsic defect structure of the layered semiconductors. Irradiation only acted as an activation factor for such processes as migration of point defects and impurities, transition of metastable states into stable ones, i.e. caused some radiation-stimulated processes. The latter did not lead to changes in the energy spectra of InSe as confirmed by the X-ray analysis and Raman spectra. At the same time, Si photodiodes irradiated under the same conditions showed a strong degradation of photoelectric parameters.

On the basis of the results of this study, the InSe photoconverters and more especially the *intrinsic oxide*–p–InSe structure, are recommended for operation under high-energy  $\gamma$ -irradiation.

#### References

- [1] Z.D. Kovalyuk, O.A. Politanska, P.G. Litovchenko, V.F. Lastovetskii, O.P. Litovchenko, V.K. Dubovoi, L.A. Polivtsev, Tech. Phys. Lett. 33 (2007) 767.
- [2] Z.D. Kovalyuk, O.A. Politanska, O.N. Sydor, V.T. Maslyuk, Semiconductors 42 (2008) 1292.
- [3] Z.D. Kovalyuk, V.N. Katerinchuk, O.A. Politanska, O.N. Sydor, V.V. Khomyak, Tech. Phys. Lett. 31 (2005) 359.

- [4] Z.D. Kovalyuk, V.M. Katerynchuk, I.V. Mintyanskii, A.I. Savchuk, O.M. Sydor, *Mater. Sci. Eng. B* 118 (2005) 147.
- [5] T. Yamazaki, H. Nakatani, N. Ikeda, *Jpn. J. Appl. Phys.* 32 (1993) 1857.
- [6] T. Yamazaki, K. Terayama, T. Shimazaki, H. Naktani, *Jpn. J. Appl. Phys.* 36 (1997) 378.
- [7] K.A. Askerov, V.I. Gadzhieva, *Proc. SPIE* 5834 (2005) 342.
- [8] K.A. Askerov, A.Z. Abasova, F.K. Isaev, *Appl. Phys.* 4 (2004) 94 (in Russian).
- [9] O.Z. Alekperov, *Inorg. Mater.* 35 (1999) 1125.
- [10] A.Z. Abasova, F.A. Zaitov, *Sov. Phys. Semicond.* 20 (1986) 390.
- [11] R.Yu. Aliev, K.A. Askerov, *Appl. Phys.* 3 (1999) 114 (in Russian).
- [12] S. Shigetomi, T. Ikari, *J. Appl. Phys.* 88 (2000) 1520.
- [13] Z.D. Kovalyuk, V.M. Katerynchuk, A.I. Savchuk, O.M. Sydor, *Mater. Sci. Eng. B* 109 (2004) 252.
- [14] N. Kuroda, Y. Nishina, *Solid State Commun.* 30 (1979) 95.
- [15] T.D. Ibragimov, E.A. Dzhafarova, Z.B. Safarov, *Semiconductors* 36 (2002) 805.
- [16] S.M. Sze, *Physics of Semiconductor Devices*, second Ed., Wiley, New York, 1981.
- [17] V.A. Manasson, A.I. Malik, V.B. Baranyuk, *Sov. Tech. Phys. Lett.* 7 (1981) 234.
- [18] M.A. Lampert, P. Mark, *Current Injection in Solids*, Academic, New York, 1970.
- [19] A.Sh. Abdinov, A.G. Kyazym-zade, N.M. Mekhtiev, M.D. Khomutova, A.G. Sharipov, *Sov. Phys. Semicond.* 10 (1976) 44.
- [20] A.M. Goodman, *J. Appl. Phys.* 34 (1963) 329.
- [21] B. Abay, H.S. Güder, H. Efeoglu, Y.K. Yogurtçu, *J. Phys. D: Appl. Phys.* 32 (1999) 2942.
- [22] B. Gürbulak, *Solid State Commun.* 109 (1999) 665.